Journal of Materials Chemistry B

Accepted Manuscript

ROYAL SOCIETY OF CHEMISTRY

www.rsc.org/materialsB

Journal Name

RSCPublishing

ARTICLE

Chitosan – alginate multilayered films with gradients of physicochemical cues

Cite this: DOI: 10.1039/xoxxoooooox

Joana M.Silva,[ab] Sofia G. Caridade,[ab] Nuno M. Oliveira,[ab] Rui L. Reis,[ab] João F. Mano *[ab]

Received ooth January 2012,
Accepted ooth January 2012

DOI: 10.1039/xoxxoooooox

www.rsc.org/

Tissues presenting continuous variations of properties in one direction have been inspired the development of functional graded materials. In this work, we developed a new facile method for the development of continuous gradients in chitosan (CHIT) and alginate (ALG) polyelectrolyte multilayers (PEMs) obtained by layer-by-layer based on the gradual dipping of CHIT/ALG coated glass slides in genipin solution. Stiffness gradients were produced in the cm scale by varying the reaction time with genipin. Quartz crystal microbalance, colorimetric measurements, trypan blue assay, attenuated total reflection - Fourier transform infrared, swelling ability, water contact angle and dynamic mechanical analysis (DMA) were used to find the suitable conditions for stiffness gradient. The PEMs can be successfully built-up and cross-linked with genipin to yield surfaces with uniform or with gradients of different physicochemical properties. It was found that a large reduction in the hydrophobic nature of the CHIT/ALG PEMs could be produced with higher cross-linking reaction times, regardless the decrease on their swelling ability. Moreover, the mechanical properties were evaluated using an innovative and non-conventional DMA to monitor crosslinking reaction *in situ*. The results confirm an enhancement on the tensile storage modulus with increasing reaction times from 60 to 140 MPa. In another original DMA testing protocol the local compression storage modulus was also measured directly on the films along the stiffness gradient, with results consistent with the tensile tests obtained on the freestanding membranes with different cross-linking degrees. The *in vitro* biological performance demonstrates that L929 adhered and spread more in the stiffer regions. This work demonstrate the versatility and feasibility of the LbL methodology to generate functional biomimetic surfaces with tuned mechanical and physicochemical properties which hold great promise for the study of cell-substrate interactions.

Introduction

Most cell types are sensitive to mechanical stimulus of the surrounding environment which affects significantly several cellular processes, including morphology, adhesion, spreading, motility, proliferation, differentiation, migration and gene expression [1-4]. The mechanical signals (matrix stiffness, elasticity and viscoelasticity) play an important role on how cells spread migrate, contract and organize key intracellular structures, such as focal adhesion [1, 5]. Thus, the use of substrates containing continuous gradients of stiffness is a current challenge for tissue engineering (TE) to mimic cellular-extracellular architecture that exists throughout the human body within tissues and at tissue interfaces [6]. Among the available techniques, layer-by-layer (LbL) appears as a promising candidate to develop graded biomimetic nanostratified systems, exhibiting such characteristics. This technique is a simple, handling, inexpensive and a powerful tool that allows the production of stratified multilayer films [7, 8]. The basic principle of this technique relies on the build-up of films based on multimode of intermolecular interactions [9-11]. For LbL based on electrostatic interactions polyelectrolyte multilayers (PEMs) films can be obtained through alternate deposition of oppositely charged polyelectrolytes which is a consequence of substrate charge overcompensation during the previous polyelectrolyte nanosized layer [12, 13]. The procedure enables the fine control of nanoscale films properties by simple adjustment of processing

parameters such as: nature of polyelectrolytes, number of functional groups, molecular weight, temperature, pH and ionic strength [9, 10, 13]. Controlling the processing parameters allows a nanometer scale control over film growth and internal structures [12, 13]. Thus, nanostructured multilayers can be obtained with tailored physicochemical, topographical and biological properties [10]. With LbL virtually any template may be employed to obtain complex structures such as: capsules [14], freestanding membranes [15, 16], hollow tubes [17] and porous scaffolds [18]. Additionally, PEMs can be used as reservoirs of biomolecules [19] as well as to functionalize surfaces, in order to mimic the natural environment of cells i.e: chemical and physical heterogeneous properties of ECM [20-24]. Gradient materials have been used to rapidly screen cell-biomaterial interaction and to study cellular processes, such as directional cell migration, adhesion mechanism, among others as aforementioned [25]. Gradients on PEMs can be generated along X or Z directions depending on the methodology used. The great majority of gradients already produced in PEMs were made in the X direction, such as the gradients of stiffness [20, 23], pH [22], and soluble factors [20]. Continuous change in swelling was achieved among the gradients produced in the Z direction [21]. However, to the date there are few examples that generate stable materials with gradients of stiffness. One of them is the use of microfluidic approaches to generate gradients of the water soluble carbodiimide on poly(L-lysine) (PLL) and hyaluronic acid (HA) multilayers [20]. Another work reported the production of multilayers with photogenerated gradients of modulus by varying the time of uniform ultraviolet light exposure or by using optical density gradient filters [23]. Herein, we propose a new straightforward dipping-based methodology able to generate gradients of PEMs properties through a perfect positional control of the cross-linking reaction time.

For the proof-of-concept chitosan (CHIT) and alginate (ALG) were used to build-up PEMs due to their potential producing reproducible and biocompatible nanolayered films [26, 27]. However, they are commonly reported to exhibit low stiffness and poor cell adhesion [28, 29]. Genipin is a natural product derived from geniposides that has been extensively investigated in cross-linking of amine-containing polymers (e.g. chitosan, collagen or gelatin) [30, 31] as well as in multilayered films [17, 28, 29, 32].[17] This natural molecule has been emerging as a favorable cross-linking agent due to its low cytotoxicity compared to the widely used glutaraldehyde (i.e. 5000 to 10000 fold less toxic compared to the glutaraldehyde) and its ability to undergo self-polymerization, which can be exploited to tailor the properties of the final constructs [31, 33]. Here, we cross-linked CHIT/ALG films with genipin. Since ALG does not contain primary amines, genipin will give rise to semi-interpenetrating polymer networks with free ALG chains entrapped inside cross-linked CHIT multilayers, as previously reported in other multilayered systems [32]. In this work genipin was used to yield surfaces with uniform or with gradients of stiffness, improving the mechanical properties and stability in physiological environment. To the date there are no reports of continuous gradients of stiffness produced by genipin cross-linking in PEMs. Scheme 1 presents the method proposed in this work to generate the gradients. It is based on the continuous increase of the level of a genipin solution along the length of a CHIT/ALG film. A series of characterization techniques are used to monitor the influence of the resulting stiffness gradient on physicochemical and biological properties.

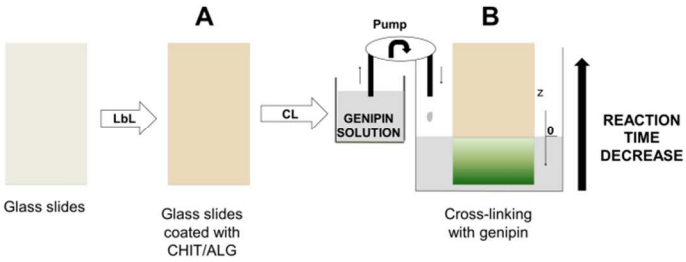

Scheme 1. Production steps of glass –coated CHIT/ALG PEMs with gradients of cross-linking. A: glass slides coated with polyelectrolytes (LbL); B: Cross-linking of PEMs with genipin where the level of genipin solution continuously increase using a peristaltic pump.

Experimental

Quartz crystal microbalance with dissipation monitoring

The two polyelectrolytes used to process the multilayers were CHIT medium molecular weight (M_w 190.000-310.000 Da, 82.6% degree of deacetylation, ref. 448877, Sigma Aldrich, USA) and low viscosity ALG (538 kDa ≈ 250 cP, ref.71238, Sigma Aldrich, USA). CHIT was purified by a series of filtration and precipitation in water and ethanol steps.

The build-up of PEMs was followed *in situ* by quartz crystal microbalance (QCM-Dissipation, Q-Sense, Sweden), using gold coated sensor excited at seventh overtone (35 MHz). The crystals were cleaned in an ultrasound bath at 30°C using successively acetone, ethanol and isopropanol. Adsorption of the different solutions took place with a constant flow rate of 100 µL.min^{-1}. The polyelectrolyte solutions were freshly prepared at a concentration of 0.2 % (w/v). For the adjustment of pH, a sodium acetate buffer (0.1 M) was prepared at pH 5.5 in the presence of additional salt (0.15 M NaCl, pH 5.5). The CHIT solution was injected standing for 6 min to allow the adsorption until the equilibrium at the crystal surface. After rinsing with sodium acetate buffer / 0.15 M NaCl (4 min), the same procedure was followed for ALG deposition. These steps were repeated to 10 double layers (dL). The conditions used for the assembly were optimized in previous works [16, 17, 34]. After the build-up the multilayers were flushed with a genipin solution (Wako chemical, USA). The solution was pumped into the system for 24 hours. A genipin solution (5 mg.mL^{-1}) was prepared by dissolving the adequate amount of lyophilized genipin into a dimethyl sulfoxide (Sigma Aldrich USA)/sodium acetate buffer (0.15 M NaCl, pH 5.5) mixture (1:4, (v/v)). The frequency and dissipation was monitored in real time. The thickness of the film was estimated using the Voigt model through the Q-Tools Software, from Q-Sense [35].

Production of freestanding membranes

Freestanding membranes were produced as reported before [16]. Briefly, polyelectrolytes solutions were alternately deposited onto a polypropylene film to form 100 dL of CHIT and ALG using a dipping robot especially designed for the automatic fabrication of multilayers. After dried at room temperature, the membranes could be easily detached from the substrate. Cross-linking of the CHIT within the multilayers was performed with genipin as aforementioned. The crosslinking agent solution was incubated with freestanding membranes during predetermined reaction times (t= 1 hour, 3 hours, 6 hours, 9 hours, 12 hours, 24 hours and 48 hours) The resultant cross-linked freestanding membranes were then rinsed in DMSO/ sodium acetate buffer (0.15 M NaCl, pH 5.5) mixture during 30 minutes, followed by a extensively washing in sodium acetate buffer. Afterwards the membranes were dried at 37 ºC overnight.

Confocal Laser Scanning Microscopy (CLSM)

Freestanding membranes were prepared with CHIT labeled with Cy 5.5 and ALG with rhodamine (Rhd), following a protocol already reported[36]. Briefly, for the CHI labeling with Cy 5.5, 10 mL of CHI solution (10 mg/mL) was prepared and a 10 mg/mL Cy 5.5 solution was prepared in DMF in dark conditions. The pH of the CHI was slowly increased to pH 6. A volume of 74.7 µL of the dye was added to the CHI solution and the mixture was protected from the light and stirred during 2 hours at RT. The pH of the mixture was acidified around pH 5 and placed in a dialysis tube always protected from the light. The dialysis tube was place in a recipient containing acetate buffer pH 5 that was changed three times per day during three days. The freestanding membranes produced with CHIT Cy 5.5/ALG Rhd were observed with an TCSP8 confocal (Leica, Germany). Images were acquired in PBS.

Production of cross-linking gradients on glass slides

A cross-linking gradient was produced in glass slides (Deltalab, Spain) previously coated with 100 layers of CHIT and ALG (0.2 % (w/v)) by using a dipping robot. The coated glass slides were dried and vertically placed inside an empty recipient (**Scheme 1**). A peristaltic pump with a controlled flow (1.8 mL per hour) was used to submerge the glass slide into a genipin solution. The sample is gradually filled with genipin solution along the vertical direction (Z) with a rate of $\dot{Z}$=dZ/dt. In the end the bottom of the sample presents the highest cross-linking which progressively decrease up to the other extreme (Z=0). The immersion time at any given point Z of the sample can be obtained by integrating dt=dZ/$\dot{Z}$

$$t(Z) = \int_0^Z \frac{dZ}{\dot{Z}} \qquad (1)$$

Note that $\dot{Z}$ can vary with Z. For the particular case of a constant dipping rate equation 1 results in t(Z)=Z/$\dot{Z}$. We opted for an average $\dot{Z}$= 0.2 cm.h^{-1} that allowed to cover the cross-linking reaction during 24 hours. The resultant graded film was then rinsed in DMSO/ sodium acetate buffer (0.15 M NaCl, pH 5.5) mixture during 30 minutes, followed by an extensively washing in sodium acetate buffer. Afterwards the glass slide was dried at 37 ºC overnight.

Scanning Electronic Microscopy (SEM)

The morphology of the freestanding membranes with different cross-linking reaction times was observed by Scanning Electronic Microscopy (SEM), using a Leica Cambridge S 360 (UK) operated at 15 kV accelerating voltage. All the samples were sputtered with a conductive gold layer, using a sputter coater SC502 (Fison instruments, UK). For the cross-section observation, the freestanding membranes were immersed in liquid nitrogen until free fracture. Three freestanding membranes were measured for each condition.

Atomic Force Microscopy (AFM) Imaging.

Dried freestanding membranes were imaged using a MultiMode STM microscope controlled by the NanoScope III from Digital Instruments system (Bruker, France) operating in intermittent contact mode. A ScanAsyst-Air cantilever (Bruker, France) with a resonance frequency of 320 kHz and a spring constant of 2 N/m was used. Substrate topographies were imaged with 512 × 512 pixels^2 at line rates of 1 Hz. For surface roughness analysis, 5 × 5 µm^2 AFM images were obtained and the rootmean squared roughness (R_{RMS}) from the principal X−Y plane was calculated. The analysis of the images was performed using Gwyddion. At least three measurements were performed in different specimens.

Determination of Cross-linking Degree

The cross-linking of CHIT within the multilayers was evaluated using the trypan blue method which has affinity to free amines [37]. The test was performed immersing the non-cross-linked and the cross-linked membranes in trypan blue 0.4% (Invitrogen, USA) diluted 50x in acetate buffer (0.15 M NaCl, pH 5.5) overnight at 37º C. The supernatant absorbance was measured at 580 nm in a microplate reader (Sinergy HT, Bio-Tek, USA). A standard curve was prepared by measuring the absorbance for a series of trypan blue solutions at different concentrations. The cross-linking degree was calculated as follows:

$$CL\,(\%) = \frac{(NH_3^+ non-Xlinked\ solution) - (NH_3^+\ Xlinked\ solution)}{NH_3^+ non-Xlinked\ solution} \qquad (2)$$

Colorimetric Assays

The CHIT within the freestanding membranes was cross-linked with genipin, using different reaction times. The kinetics of cross-linking was evaluated by colorimetric assays. Color changes in samples due to chemical cross-linking were recorded by a digital camera (Nikon G12) and pixels intensity

were further quantified by colorimetric assay using *Image J* software. The measurements of the pixel intensity from each membrane conditions were performed over a total of 6 samples. The intensity of the pixels was recorded within the grey scale between 0 and 255, in which 0 correspond to dark color and 255 white color.

Fourier Transform Infrared (FTIR) Spectroscopy

FTIR measurements were recorded using an IR-Prestige-21 spectrophotometer (Shimadzu Scientific Instruments, USA) by averaging 34 individual scans over the range from 2000 cm^{-1} to 800 cm^{-1}. CHIT/ALG and cross-linked freestanding membranes were analyzed in attenuated total reflection (ATR) mode.

Water Contact Angle (WCA)

The wettability of the studied freestanding membranes was characterized by WCA measurements. Static WCA measurements were performed using the sessile drop method on an OCA15+ goniometer (DataPhysics, Germany) under ambient conditions at room temperature. Milli-Q water (6 µL) was dropped onto the membranes and pictures were taken after water drop stabilization. The WCA was also measured at different positions of the films along the gradients of stiffness. Three samples of each formulation were measured five times.

Water - uptake

The water-uptake ability of the freestanding membranes with and without cross-linking was measured soaking dry films with known weight in acetate buffer (0.15 M NaCl, pH 5.5) or acetate buffer (0.15 M NaCl, pH 5.5) / DMSO. The swollen films were removed after predetermined time points (t=15 min, 30 min, 1 h, 3 h, 5 h,8 h, 12 h, 24 h and 48 h). After removing the excess of solution using a filter paper (Filter Lab, Spain), the freestanding films were weighed with an analytical balance (Denver Instrument, Germany). The water uptake was calculated as followed:

$$Water\ uptake\% = \frac{W_w - W_d}{W_d} \times 100 \quad (3)$$

where W_w and W_d are the weights of swollen and dried freestanding films, respectively.

Mechanical Tests

All viscoelastic measurements were performed using a TRITEC2000B DMA from Triton Technology (UK), equipped with the tensile mode. The measurements were carried out at 37°C. Freestanding membranes were cut in samples with about 5 mm width (measured accurately for each sample). Two different experiments were performed: one was in real-time and the other one was offline. In the online experiments, the freestanding membranes were immersed in acetate buffer (0.15 M NaCl, pH 5.5) until equilibrium was reached. After measuring the geometry, the samples were clamped in the DMA apparatus and immersed in the genipin solution or in control solutions (acetate buffer (0.15 M NaCl, pH 5.5) or acetate buffer (0.15 M NaCl, pH 5.5) / DMSO) bath at 37ºC. Tensile experiments were carried out at 1 Hz, with constant strain amplitude of 30 µm. The offline experiments were performed by measuring membranes with and without cross-linking in different solutions: acetate buffer (0.15 M NaCl, pH 5.5) and acetate buffer (0.15 M NaCl, pH 5.5) / DMSO. The DMA spectra were obtained during a frequency scan between 0.1 and 20 Hz. The experiments were performed using a constant amplitude strain of 30 µm. Three specimens were tested for each condition.

The mechanical properties along the continuous gradient were also evaluated using a non-conventional "micro-compression" DMA approach. A micropillar with a cross-section of 4.98 mm^2 was inserted in the DMA apparatus in order to allow non-destructive compression measurements in discrete points of the gradient. The film could be moved along the X direction to be probed at different positions. Tests were performed using different displacement amplitudes from 0.5 to 10 µm. Upon optimization, a displacement of 2 µm was used for the majority of the tests. The experiments were performed in acetate buffer bath at 37ºC. DMA spectra along the continuous gradients were obtained during a frequency scan between 0.5 and 20 Hz.

Cell Culture

To evaluate the biological performance of CHIT/ALG and cross-linked CHIT/ALG freestanding membranes, cell culture studies were performed with L929, a mouse fibroblast of connective tissue cell line (European Collection of Cell Cultures (ECCC), UK). Cells were cultured in Dulbecco's modified Eagle's medium (DMEM; Sigma, USA), supplemented by 10% heat-inactivated fetal bovine serum (FBS; Biochrom AG, Germany) and 1% antibiotic- antimicotic (Gibco, USA). Prior to cell seeding, membranes were sterilized with 70% (v/v) ethanol overnight and then rinsed three times in PBS, whereas surfaces were treated with ultraviolet (UV) light to avoid the damage of the coating (detachment of the PEMs from the glass surface due to dehydration). CHIT/ALG and cross-linked CHIT/ALG membranes were incubated for 1, 3, and 7 days at 37ºC in a humidified 5% CO_2 atmosphere. For the glass slides with cross-linking gradients L929 were seeded and their behavior was evaluated after 1 day of culture. 4,6-Diaminidino-2-phenylindole-dilactate (DAPI, 20 mg.mL-1, Sigma-Aldrich, USA) and phalloidintetramethylrhodamine B isothiocyanate dyes (phalloidin, 10 mg.mL-1, Sigma-Aldrich, USA) were used to perform a DAPI–phalloidin assay. Briefly at each time point, culture medium was removed and the samples fixed in 10% formalin. After 1 hour, formalin was removed and replaced by PBS. Upon PBS washing, 1 mL of PBS containing 10 µL of phalloidin was added for 40 minutes at room temperature and protected from light. After extensively

washing, samples were stained with 1 µl of DAPI in 1mL of PBS for 10 minutes. After DAPI staining samples were washed three times with PBS and visualized in the dark by inverted fluorescent microscope (Zeiss, Germany). The images obtained were analyzed using Image J software.

Statistical analysis

The experiences were carried out in triplicate otherwise specified. The results were presented as mean ± standard deviation (SD). Statistical analysis was performed by Shapiro Wilk normality test using Graph Pad Prism 5.0 for Windows. After this analysis, non-parametric (Kruskal Wallis test) or parametric tests (one way Anova followed by Turkey test) were used depending if the samples were from normally distributed populations or not, respectively.

Results and Discussion

Construction of CHIT/ALG multilayers

The assembly of CHIT/ALG multilayers was monitored *in situ* with QCM-D. This technique detects the adsorbed mass of polyelectrolytes and measures the viscoelastic properties of the surface [38]. Figure 1A shows the build-up of 10 bilayers in terms of variations on normalized frequency, $\Delta f_7/7$ and dissipation, ΔD_7. As expected, the normalized frequency decreases upon each injection of polyelectrolyte solution, reflecting the increase of mass over the gold sensor. The increase of ΔD_7 is due to the enhanced viscoelastic nature of the adsorbed layer structure of the deposited film. During the washing step, after the injection of each polyelectrolyte, the change of both $\Delta f_7/7$ and ΔD_7 are relatively small, indicating a strong association of the layers on the surface. The thickness of the film was estimated using the *Voigt* model instead of Sauerbrey model [35]. The Sauerbrey model is applied when a thin and rigid film of mass Δm is adsorbed at the crystal and the measurements are conducted in air [26, 39]. For viscoelastic materials the adsorbed mass does not fully couple to the oscillation of the crystal and dampens the oscillation; in this case the use of the *Voigt* model is more appropriate [26, 35]. Additionally, the decrease in the normalized frequencies ($\Delta f_n/n$) for the six overtones is clearly different, revealing that the adsorbed layer does not obey the *Sauerbrey* equation [26] (Figure 1B).

Figure 1C shows that the thickness of CHIT/ALG multilayers increases as the number of layers increase, presenting a linear growth, as previously reported [26, 27]. A thickness of ca. 250 nm was estimated for the final 10 bilayers. Regarding the layer thickness corresponding to each polyelectrolyte it was found that both have equal contributions along the build-up of PEMs.

To stabilize the CHIT/ALG films genipin was used as cross-linker and the QCMD response evaluated – see Figure S1. The CHIT/ALG multilayers were built at pH 5.5 and then incubated in 5 $mg.mL^{-1}$ genipin solution. The QCM measurements demonstrate that CHIT/ALG films cross-linked with genipin could be successfully used to conceive stable PEMs.

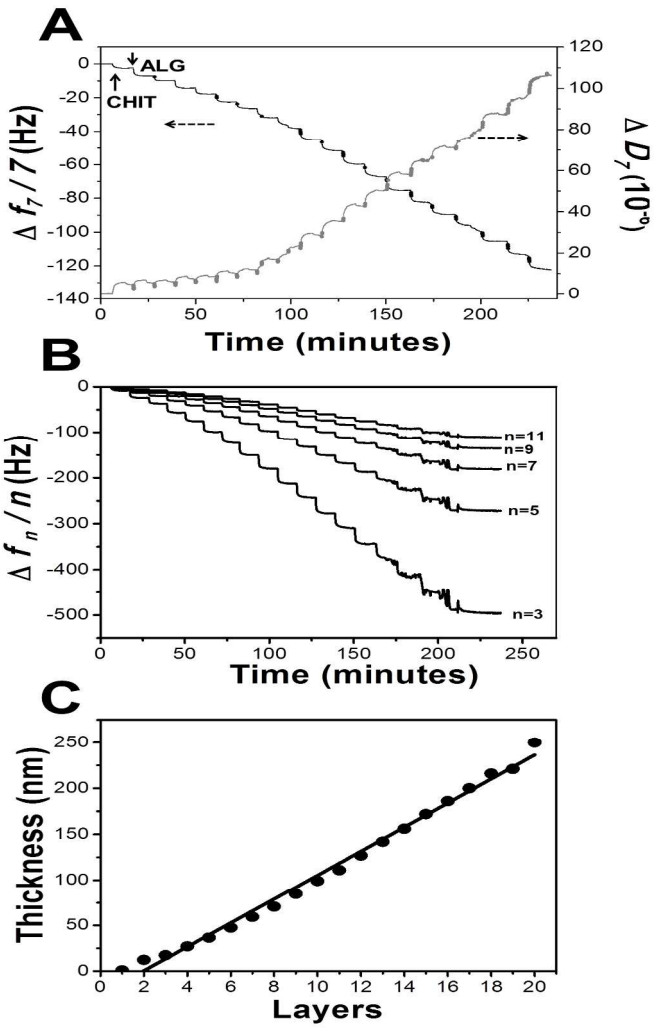

Fig 1. Monitoring of the build-up of the polyelectrolyte multi-layered CHIT/ALG films using QCM-D. A: Normalized frequency ($\Delta f_{7/7}$) and dissipation changes (ΔD_7) obtain at 35 MHz. B: Normalized frequency ($\Delta f_{n/n}$) for the five overtones (n=3, 5,7, 9 and 11. C: Cumulative thickness evolution of polymeric film as a function of the number of deposited layers. The line represents a linear regression with R^2=0.9922.

CHIT/ ALG multilayered films: physicochemical characterization

Morphology

Freestanding membranes were easily detached from polypropylene supports due to their hydrophobicity and weak interactions between the initial layer and the substrate [16]. Using these assembly parameters the membranes are robust and easy to handle such characteristics allow to cut the freestanding membranes in virtually any shape (Figure S2). The morphology of the developed CHIT/ALG membranes was evaluated by scanning electronic microscopy (SEM) - see micrographs in Figure 2A.

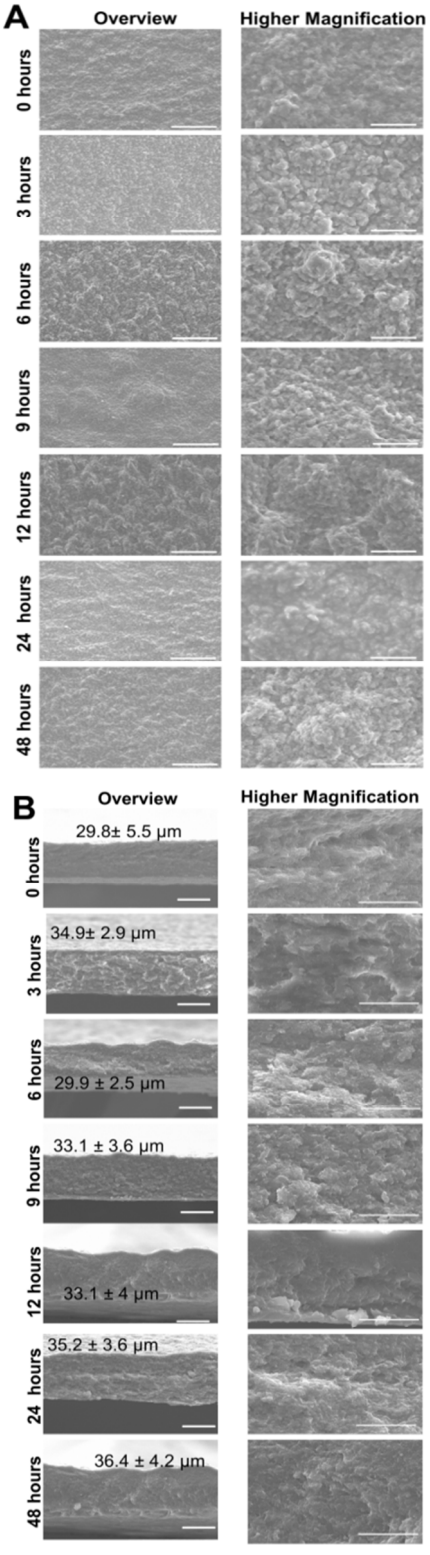

Fig 2. Morphology of freestanding membranes. A: SEM micrographs of the surface CHIT/ALG films after different crosslinking reaction times. The scale bar is 100 µm and 20 µm, for the overview and higher magnification images, respectively. B: Cross-section micrographs of the different freestanding membranes. The scale bar is 20 µm and 10 µm, for overview and higher magnification, respectively.

The results reveal an homogeneous deposition of multilayers and the absence of defects which reveal the efficacy of the detachment of the multilayers using these supports. It should be pointed out that the SEM analysis was made using the upper part of the membrane (ALG side), since as previously reported the substrate side (side in contact with the substrate prior to the detachment) is smoother [16]. The morphology of the films cross-linked with genipin at different reaction times was evaluated. The results reveal a similar morphology between the samples subjected to different reaction times and the native freestanding membrane.

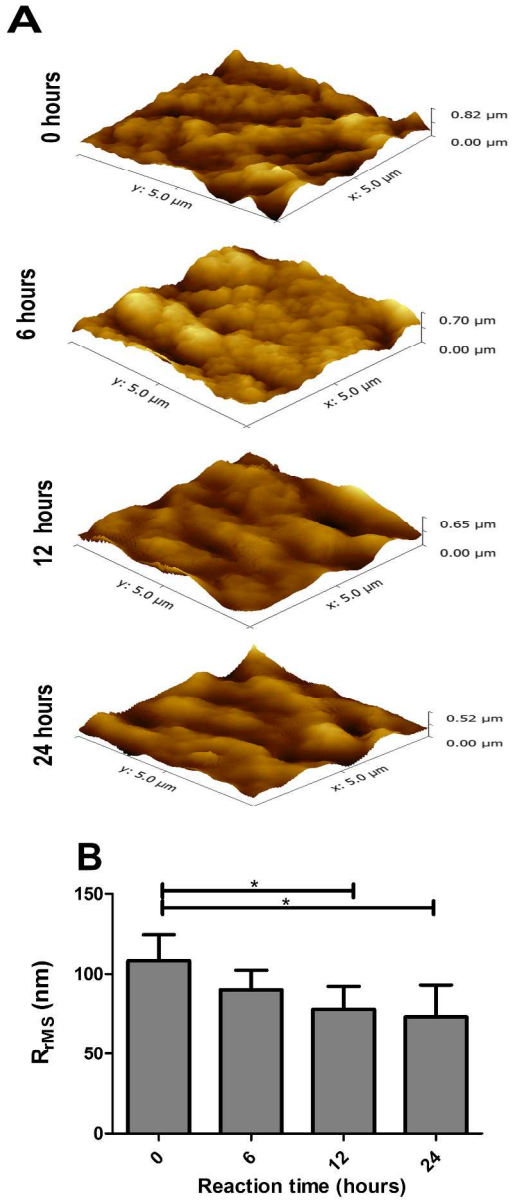

Fig 3. A: Atomic force microscopy images (5 µm2 ×5 µm2) of CHIT/ALG membranes upon different cross-linking reaction time; B: roughness analysis. Significant differences were found for (*) $p < 0.05$.

The thickness of the freestanding membranes was determined using cross-section images for all the freestanding membranes

formulations (Figure 2B). CHIT/ALG membranes present a dry thickness of 29.5 ± 5.5 µm. On the other side, membranes cross-linked have a slightly increase on the thickness up to ca. 36 ± 4.2 µm. These results are in concordance with earlier studies where the cross-linking increase the stiffness of the multilayers without significant changes of PEMs thickness in the dry state [17]. The cross-sections of all the freestanding membranes also reveal a homogeneous morphology and some porosity which is important for the diffusion of the nutrients for cells. The diffusion properties of the membranes were already reported in previous studies[16, 17]. To have a better perception of the films morphology at a lower scale we also performed AFM imaging of the surface of the films – see Figure 3. The roughness results were concordant with previous studies since a decrease in roughness occurs with an increase of cross-linking reaction time[17]. AFM imaging reveals that coating was homogenous and the values of roughness matched the ones of previous studies [17, 29]. All the formulations exhibit a rough surface, represented by submicrometer-sized islets over the surface. After crosslinking the film preserved its structure but a decrease of roughness occurs which turns the films more uniform.

Finally to further confirm the internal organization of the multilayers upon cross-linking CHIT and ALG were labeled with Cy 5.5 and Rhd, respectively, and the films were observed by confocal microscopy – see Figure 4. The results confirmed the presence of both polyelectrolytes after cross-linking with genipin. Moreover, the results also confirmed the decrease of roughness upon cross-linking which corroborated the AFM results.

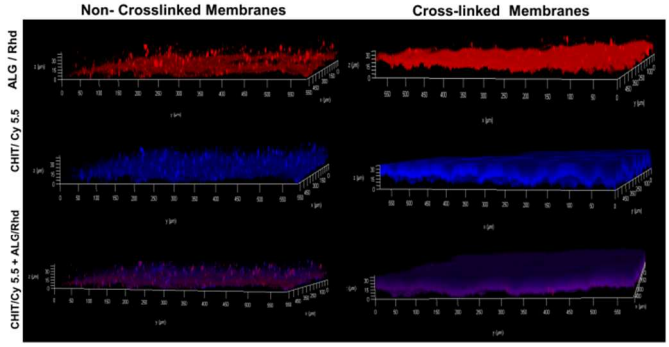

Fig 4. CSLM observations of the CHIT/ALG freestanding membranes before and after genipin cross-linking.

The concept was transposed for CHIT/ALG coated glass slides and stiffness gradients were generated using a simple and versatile methodology that allows the creation of graded materials at the cm scale. The main advantage of using this methodology when compared with others already reported in the literature is that the CHIT/ALG multilayers with stiffness gradients coated in the glass slides can be easily detached while immersed in water (Figure 5). Thus there is no need to have the multilayers permanently attached to the substrate which would limit their applications. The creation of long-range gradients will be particularly relevant for screen cell-material interactions since a large number of conditions can be tested. Additionally, the use of higher cell number increase the accuracy and finally, it reduces the number of expensive [20].

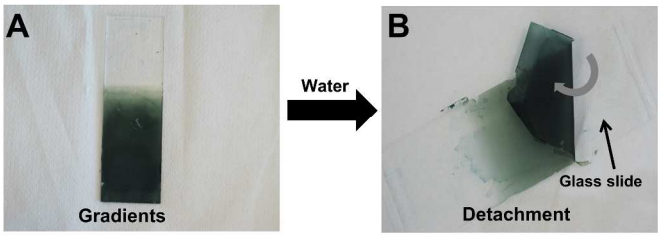

Fig 5. A: Micrograph showing a $(CHIT/ALG)_{100}$ coated glass slides after the generation of the gradient of stiffness. B: The multilayers are easily detached when immersed in water.

Cross-linking degree

Genipin has the ability to crosslink polymers containing amine-groups[30, 31]. Additionally, it has the ability to generate both color and fluorescence when reacting with primary amine groups [40]. Several works reported the aforementioned effects which can be explained by oxygen-radical induced polymerization of genipin, as well as with its reaction with amine groups[41, 42]. The trypan blue assays were performed to determine the cross-linking degree of the CHIT within the membranes, by using the same genipin concentration (5 $mg.mL^{-1}$) and different reaction times (Figure 6A). Trypan blue is a dye with the ability to bind to free amines, leading to changes in the blue colour intensity of the supernatant solution [37]. Using this principle, native and cross-linked membranes were incubated in trypan blue solution and the absorbance of the supernatant was measured. As expected, the absorbance of the supernatant increases with increasing cross-linking reaction time, since the free amine groups also decrease (inset image of Figure 6A). The cross-linking degree was calculated using a trypan blue standard curve, since the absorbance of trypan blue solution is proportional to the concentration of free amines. Thus, the absorbance of the supernatant can be compared to the absorbance present in the trypan blue solutions at different concentrations. Furthermore, it should be pointed out that during the determination of free amines it was assumed that CHIT and ALG are presented in the same proportions, which was concluded by the linear growth of CHIT/ALG obtained during QCM measurements (Figure 1C). Afterwards the cross-linking degree was determined comparing the free amines presented on the CHIT/ALG membranes with the ones present on the cross-linked membranes. The cross-linking degree could be varied from 9 % to 80 % by simple adjustment of the cross-linking reaction time.

Genipin cross-linking is well known to induce colour on the samples and the intensity of colour has been reported to be proportional to the extension of the reaction [43, 44]. Following this principle, the cross-linking was monitored by image

analysis, through pixels quantification. Figure 6B shows the evaluation of pixels intensity and the different colours obtained on the freestanding membranes. The pixels intensity changes along the time due to a gradual colour change from light to dark green. The maximum colour intensity corresponds to membranes cross-linked during 48 hours of reaction, which in turns present the lowest pixels intensity. The evolution of pixels intensity was further used to estimate the relation between cross-linking degree and the greenish colour of samples. The profile presented in Figure $6B_1$ demonstrate that the pixels intensity increase linearly with the cross-linking degree, indicating that by simple image analysis it is possible to estimate the cross-linking extent of CHIT/ ALG multilayers with genipin. The results of trypan blue assay and colorimetric measurements demonstrate that genipin is an efficiently cross-linker for CHIT/ALG multilayers.

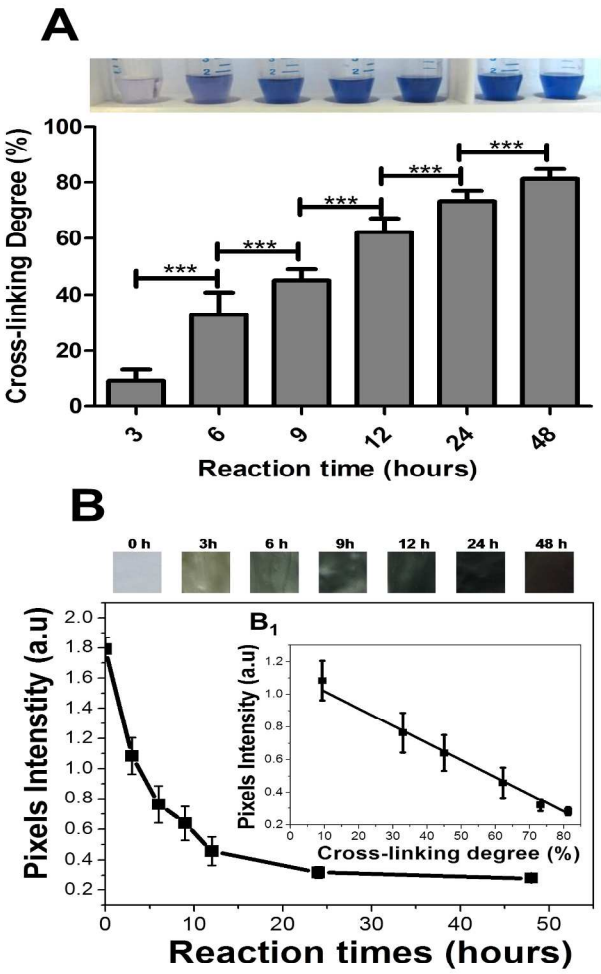

Fig 6. A: Cross-linking degree for CHIT/ALG membranes with different reaction times. The inset image represents the colour of supernatant after trypan blue assay Significant differences were found for (***) $p < 0.001$. B: Colorimetric monitoring of CHIT/ALG membranes upon cross-linking with genipin. The inset image (B1) represents the evolution of pixels intensity as a function of the cross-linking degree. The line represents a linear regression with $R^2 = 0.9931$.

ATR-FTIR Analysis of films

ATR-FTIR measurements were performed on the CHIT/ALG and cross-linked membranes – see Figure 7A. The spectra of CHIT/ALG membranes present the characteristics peaks of CHIT and ALG (Figure S3).

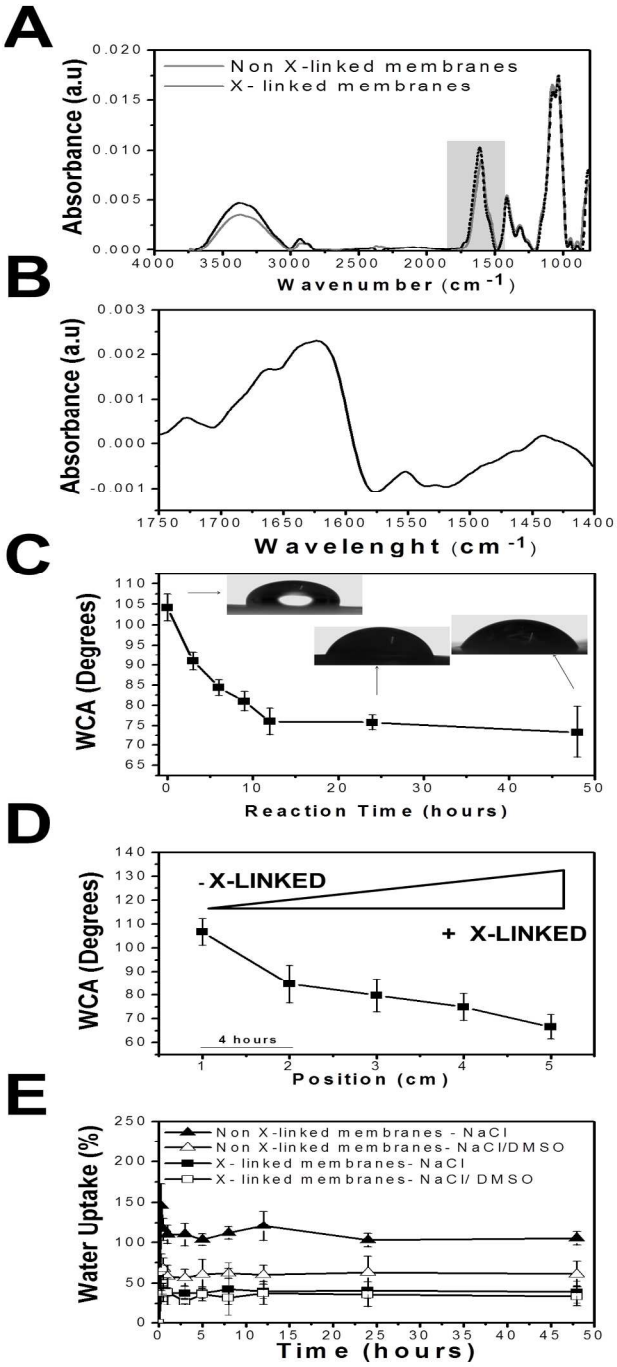

Fig 7. Physicochemical characterization of the freestanding films. A: ATR-FTIR spectra of CHIT/ALG (Non X-linked) and cross-linked (X-linked) membranes; B: Difference spectrum between X-linked membranes and Non X-linked membranes, in the region between 1750- 1400 cm^{-1}; C: Water contact angle (WCA) as a function of cross-linking reaction times, including representative droplet profiles; D: WCA along the continuous gradient; E: Swelling ability of CHIT/ALG (Non X-linked) and cross-linked (X-linked) membranes in acetate buffer (0.15 M, pH 5.5) and acetate buffer (0.15 M, pH 5.5)/DMSO.

The two polysaccharides share some common peaks between 950–1200 cm^{-1} representative of the skeletal vibration of CHIT and ALG saccharide rings [16, 26]. Two other regions can be observed in CHIT/ALG membranes spectrum: the band at 1606 cm^{-1}, attributed to –COO– asymmetric stretch from ALG and the band at 1420–1500 cm^{-1} corresponding to the amide II of CHIT [16, 26]. The spectrum of cross-linked membranes evidenced the chemical changes occurring during the cross-linking reaction. In order to make these changes more perceptible a difference between the spectra of a cross-linked membrane and a native membranes are also represented in the region of interest (Figure 7B). The resulting curve exhibits an increase in the amide I (1600-1659 cm^{-1}) and amide II (1400-1500 cm^{-1}) due to the interactions of amine groups of chitosan and ester groups of genipin which gives rise to amide bonds formation [32, 44-46]. Moreover, the difference in the two spectra demonstrate the displacement of the amide characteristic peak, an decrease in the amine peak at 1575 cm^{-1} and an increase in the peak at 1560 cm^{-1} due to the formation of alkene bonds (C=C) [28, 44]. The appearance of the band at 1700-1750 cm^{-1} could be attributed to the ester groups of genipin [28]. Another characteristic peak for genipin can be found at 1450 cm^{-1}, corresponding to the methyl group deformation [32]. All together, the spectra show, globally, the absorption peaks from both CHIT, ALG and genipin which is again indicative of the presence of both raw materials in the final structure, as well as, the efficiency of genipin cross-linking

Water contact angle

The wetting behaviour of the different freestanding membranes was evaluated by water contact angle (WCA) measurements. Figure 7C shows that CHIT/ALG freestanding membranes are hydrophobic, presenting a WCA around 100º. However, the WCA gradually decreased and the freestanding membranes become more hydrophilic with the increase of the cross-linking reaction time. The effect of reaction time with genipin has been reported for capsules [43] and hydrogels [40] but to the best of our knowledge there are no detailed studies of this process in multilayered films. The genipin crosslinking is well known to affect the surface chemistry of the materials due to their chemical derivatives. It has been reported that genipin acts through a ring opening reaction by nucleophilic attack of the CHIT amine groups. Basically the mechanism can be briefly explained as a nucleophilic attack at C-3 of genipin through the amine groups at C-2 of CHIT, resulting in the opening of the dihydropyran ring and the formation of a heterocyclic amine [40-42]. Subsequent steps involve radical-induce polymerization that create genipin heterocyclic conjugates. Additionally, the ester groups of genipin can react with amine groups in CHIT and secondary amide linkages can be established. This cross-linker presents highly selectively and it only targets amine groups. Thus, the hydroxyl and carboxylic groups did not react and in the end this reaction cross-linked CHIT chains and introduces monomers and further dimerizations within the film. These derivatives are richer in hydrophilic groups such as amine, amides and hydroxyl groups [40-42]. Since, this is a moderate reaction when compared with the one of glutaraldehyde a slowly decreasing in the hydrophobicity was observed, as the reaction time increases[40-42]. The finding was concordant with earlier studies who found a decrease of WCA in CHIT-ALG multilayers and CHIT hydrogels after crosslinking [29, 40]. The decrease has been reported to be related with the increase of cross-linker conjugates within the films. Moreover, PLL/HA multilayers cross-linked with EDC/NHS also presented a decrease in hydrophobicity with the increase of cross-linker concentration [47]. The WCA measurements were also performed along the graded glass slides and the same trend was observed (Figure 7D). In the bottom of the glass slide (stiffer region) the WCA is lower and a continuous increase occurs until the top.

Swelling ability

CHIT/ALG freestanding membranes are composed by polyelectrolytes with abundant hydrophilic groups, such as hydroxyl, amine, and carboxyl groups, which can promote water-uptake [48, 49]. The swelling ability was evaluated in acetate buffer (0.15 M NaCl, pH 5.5) and acetate buffer (0.15 M NaCl, pH 5.5) / DMSO at 37 °C during 24 hours using freestanding membranes (Figure 7E). The results showed that the water uptake increases mainly during the first 15 minutes and then stabilizes, reaching the equilibrium. The same trend is observed in samples with or without cross-linking. Non-cross-linked membranes have a higher water uptake in both solutions ≈ 105.25 % ± 8.30 % (acetate buffer (0.15 M NaCl, pH 5.5) and ≈ 61.11 % ± 15.95 % acetate buffer (0.15 M NaCl, pH 5.5) / DMSO when compared with the cross-linking ones: ≈ 38.86 % ± 13.56 % and 33.72 % ± 12.87 %, respectively. Moreover, the swelling of membranes with and without cross-linking decreases when the solution contained DMSO. The cross-linking with genipin led to lower water-uptake due to the smaller intermolecular space between the polyelectrolyte chains. Such effects are the ones that are classically reported in hydrogel systems. With the increasing of cross-linking, despite the water-uptake decreases the apparent hydrophilicity increases. This could be explained by the existence of hydrophilic groups in the genipin structure that will bridge the CHIT chains. These results are further corroborated with the ones in the literature [30, 40] and with the mechanical properties.

Mechanical properties

Dynamic mechanical analysis (DMA) is an adequate technique for characterizing the mechanical properties of biomaterials, as it can use test conditions that closely stimulate the physiological environment [50]. Performing mechanical test on biomaterials with water-uptake ability under physiologically–like conditions is of major importance, since it has been proved that material tested in buffered solution at 37ºC exhibit a completely different viscoelastic behavior to the one observed

in dry conditions [50]. In this work, online DMA experiments were performed for the first time on freestanding multilayered films to monitor the cross-linking reaction *in situ*. The motivation for this experiment is that if the cross-linking reaction time of genipin affects the physicochemical properties of the freestanding membranes, its mechanical properties will also continuously change. DMA experiments were used to monitor the change in the viscoelastic properties of the samples immersed in acetate buffer (0.15 M NaCl, pH 5.5), acetate buffer (0.15 M NaCl, pH 5.5)/DMSO, and acetate buffer (0.15 M NaCl, pH 5.5) DMSO/ genipin. Acetate buffer (0.15 M NaCl, pH 5.5) and acetate buffer (0.15 M NaCl, pH 5.5)/DMSO were used as control media in order to evaluate the effect of these solvents during cross-linking reaction (Figure 8). The values of storage modulus (*E'*) and loss factor (*tan* δ) are shown as a function of time (Figure 8A and Figure 8B).

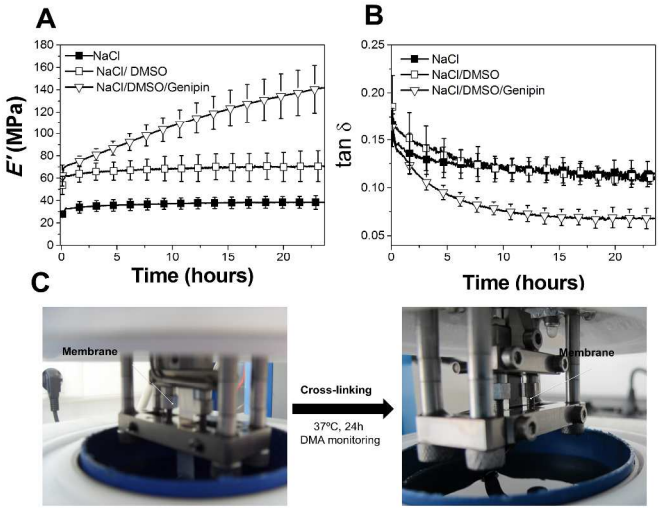

Fig 8. Online DMA measurements at 1 Hz. A, B: Variations of Storage modulus (*E'*) and loss factor (tan δ) of CHIT/ALG membranes while immersed in acetate buffer (0.15 M, pH 5.5), acetate buffer (0.15 M, pH 5.5)/DMSO and acetate buffer (0.15 M, pH 5.5)/DMSO/Genipin solutions at 37°C. C: Pictures evidencing the membranes alterations during the cross-linking followed in the DMA equipment.

Freestanding membranes immersed on acetate buffer and acetate buffer/DMSO present a similar behavior since *E'* and tan δ remain stable along the time. However, the *E'* is higher on acetate buffer/DMSO, since DMSO is an organic solvent that decrease the water-swelling ability of the membranes (see section of swelling ability), increasing their stiffness. A higher *E'* was already reported before for solvent casted membranes based on chitosan when immersed in ethanol solution [51]. On the other hand, the membranes immersed in acetate buffer/DMSO/genipin present a continuously increase in *E'* accompanied by a continuously decrease on tan δ. The increase in *E'* up to ca. 24 hours corroborated the stiffening effect generated upon cross-linking with genipin. The tan δ is the ratio between the energy lost by viscous mechanisms and the energy stored in the elastic component, providing information about the damping properties of the material [52]. The decrease in *tan* δ indicates that the membranes acquire more elastic properties during cross-linking accompanied by a release of water molecules.

The results were further compared with the ones performed during offline experiments, using non-cross-linked and cross-linked membranes (after 24 hours of reaction) immersed in acetate buffer (0.15 M NaCl, pH 5.5) and acetate buffer (0.15 M NaCl, pH 5.5)/DMSO (Figure 9A and Figure 9B). The results at 1 Hz are concordant with the ones obtained in online experiences. However, the values from the offline experiments are lower. Thus, the results suggested that the cross-linking is further enhanced by cyclic mechanical stimulus imposed to the samples during the online experiments. The same behavior was reported in literature for biomineralization processes, followed also *in situ* with DMA [50].

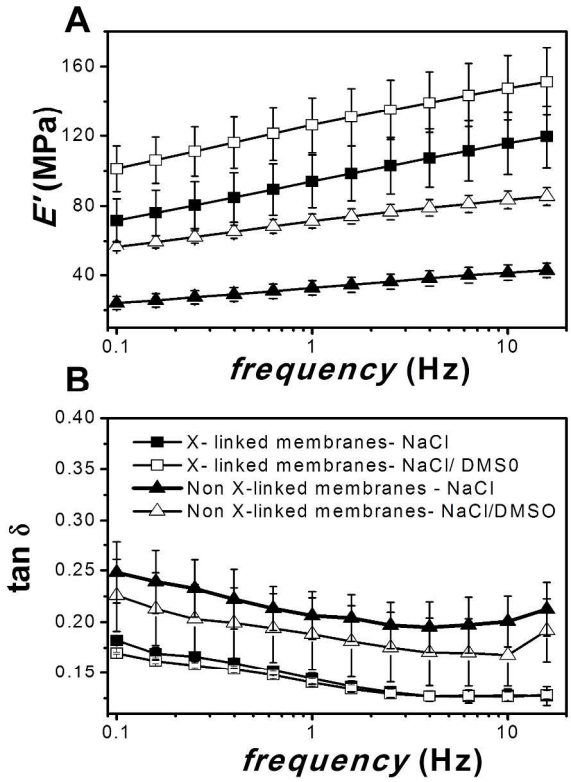

Fig 9. Offline DMA measurements: DMA scans of non-cross-linked membranes and cross-linked membranes obtained under immersion in acetate buffer (0.15 M, pH 5.5) and acetate buffer (0.15 M, pH 5.5)/DMSO at 37°C. A, B: Storage modulus (E') and loss factor (tan δ).

DMA analysis on CHIT/ALG freestanding membranes showed that crosslinking reaction time influences the mechanical/viscoelastic properties of the multilayers. Surfaces with continuous gradients of stiffness were also produced and their mechanical properties evaluated with a non-conventional local "*micro compression*" DMA analysis (Figure 10 A). This approach is an innovative and non-conventional approach which allows the direct measurement of mechanical properties along the stiffness gradient.

The apparent modulus (E_a) increases along the length of the glass slide within a range of 17 – 98 MPa – see Figure 10 B. The continuously increase of modulus along the stiffness gradient corroborated the premise that stiffening effect generate by genipin crosslinking is dependent on the reaction time. Additionally, using this approach the viscoelastic properties of the PEMs were also assessed with tan δ. The increase of modulus was accompanied by a decrease on tan δ. The decrease of tan δ occurs due to the release of water molecules upon higher cross-linking reaction time and, consequently, higher cross-linking degree. The same trend was verified during the frequency scan i.e. the E_a increase as the reaction time increase (increase position on the gradient) and the tan δ decrease (Figure S4 A and B). The efficiency and sensibility of this technique was further confirmed using different amplitude of displacements. The results reveal that the displacement should be between 0.5 - 2 µm. With a higher displacement the E_a increase and reach the equilibrium due to the effect of the stiff substrate (glass slide) - see Figures S4 C. Altogether, the results of "*micro-compression*" confirm the successful generation of stiffness gradient.

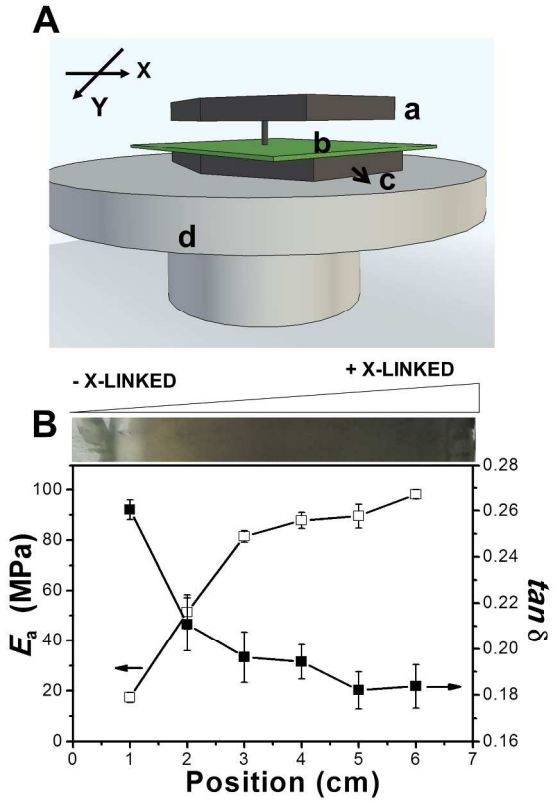

Fig 10.. Non-conventional local DMA "micro-compression" tests. A: Schematic representation of the operational setup: a: adapted indentation probe for the microcompression test; b: sample film; c: Movable XY support for the sample; d; DMA bottom plate for compression tests. B: Variations of apparent modulus (E_a) and loss factor (tan δ) as a function of the position on the gradient. A micrograph showing the change of the color of the films is shown on top.

Biological performance

In vitro tests were performed on native and cross-linked membranes with 100 bilayers of CHIT and ALG was evaluated *in vitro* with L929 cells. Cell adhesion and morphology was studied by DAPI-phalloidin assay (Figure 11A).

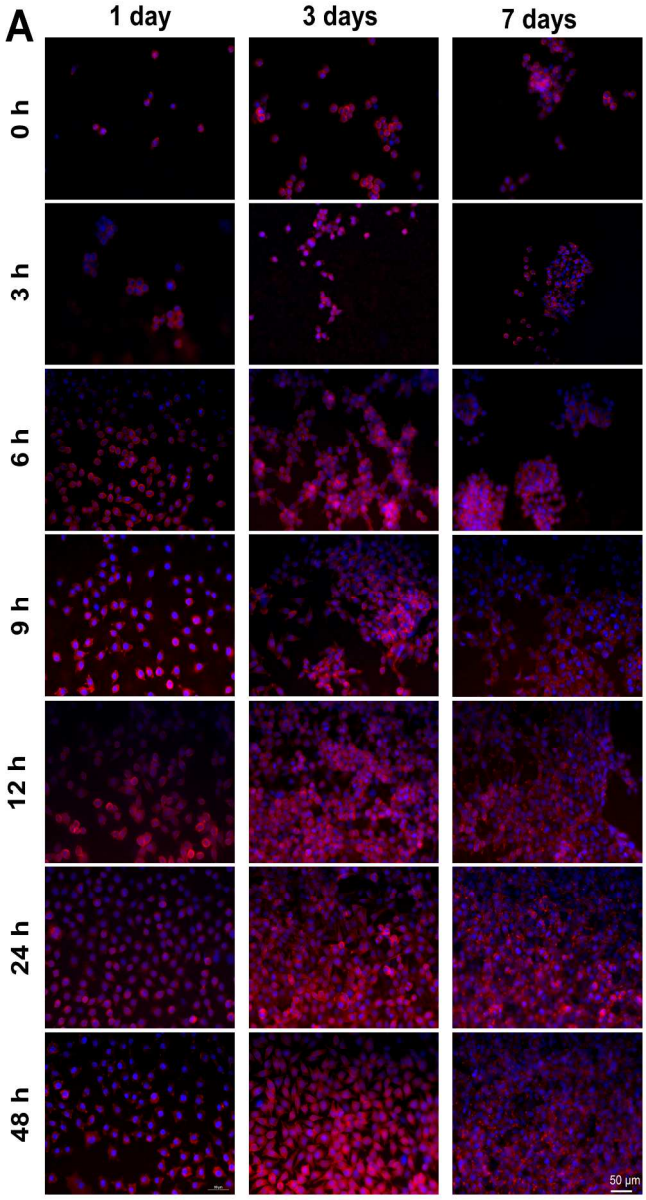

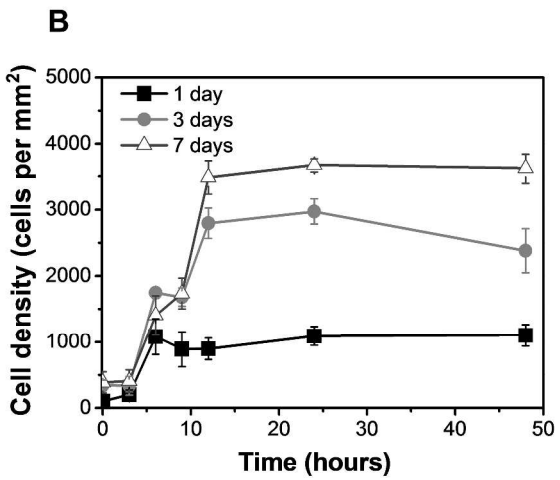

Fig 11. A: DAPI-phalloidin fluorescence assay at 1, 3, and 7 days of culture on CHIT/ALG and cross-linked CHIT/ALG freestanding films. Cells nuclei were stained in blue by DAPI and F-actin filaments in red by phalloidin. Scale bar represents 50 µm. B: Cell density at 1, 3 and 7 days of culture on all freestanding films formulations.

Cells seeded on membranes adhere on the surface but behave quite different between the formulations. As expected, the cross-linking has a positive effect on cell adhesion but the effect is only noticeable after 6 hours of reaction. With a cross-linking reaction time higher than 6 hours (> 30% cross-linking degree) cells are well spread and anchored to the film, presenting a stretched morphology. A noticeable increase in cell number occurs between 9 hours and 12 hours and then become stationary, corroborating the cross-linking degree results. On the other side, the cells cultured on native and slightly cross-linked membranes are less susceptible to create strong anchors which can occur due to the softness and high hydration of these films. The cells seeded on these films tend to aggregate, presenting a round morphology. With these results it is also possible to verify an increase in cell number with increasing culture time, as well as the influence of cross-linking reaction time on cell adhesion and proliferation (Figure 11B). Moreover, after 3 days of culture most of the surface area is covered with exception to the native films and films with lower cross-linking reaction times. The behavior is even more pronounced after 7 days where the surface area is completely covered by cells and confluence is over-achieved. Thus, on higher cross-linked membranes, cells proliferate in dense layers, whereas on native membranes they are organized in clusters. Clusters have been widely reported as prominent in cases of deficient cell-matrix interactions, which protect them against anoikis that is apoptosis induce by poor adhesion [53].

After the preliminary studies performed on freestanding membranes, the concept was transpose to glass slides with gradients of stiffness. L929 cell line was also used as a cell model and DAPI – phalloidin assay was performed to evaluate cell behavior (Figure 12A). The results are consistent with the ones obtained in the freestanding membranes. Glass slides coated with native films are unfavorable for cell adhesion, thought the positive effect of cross-linking is strongly dependent on the reaction time. Whereas only few cells remain on the cross-linked film with lower reaction times, the number of cells significantly increases as the reaction times increase (Figure 12B). Thus, cell number and adhesion is found to be highly correlated with the cross-linking reaction time which affects the wettability and stiffness of the films. The wettability affects cell adhesion and it is universally accepted that cells adhered better to moderate hydrophilic surfaces in comparison to hydrophobic or hydrophilic extremes [29]. Additionally, the chemical cross-linking is well known to increase the stiffness, decreasing its water content, which is a property also responsible to modulate specific cellular events [29]. The continuous gradient generated from the bottom to the top of the film present an increase of hydrophilicity and stiffness that affects the cell behavior. This behavior is consistent with other studies reported in literature for other types of cells (fibroblasts, smooth muscle cells and neurons) using different PEMs [47, 54, 55]. Cross-linking is a known mechanism to tailor the properties of PEMs which plays a role in many cellular processes ranging from motility, to spreading, proliferation and differentiation [46, 54, 56]. Gathering all the results, this study demonstrates the important role of surfaces with continuous gradients of physical cues generated by varying the reaction time of genipin cross-linking in cell adhesive properties.

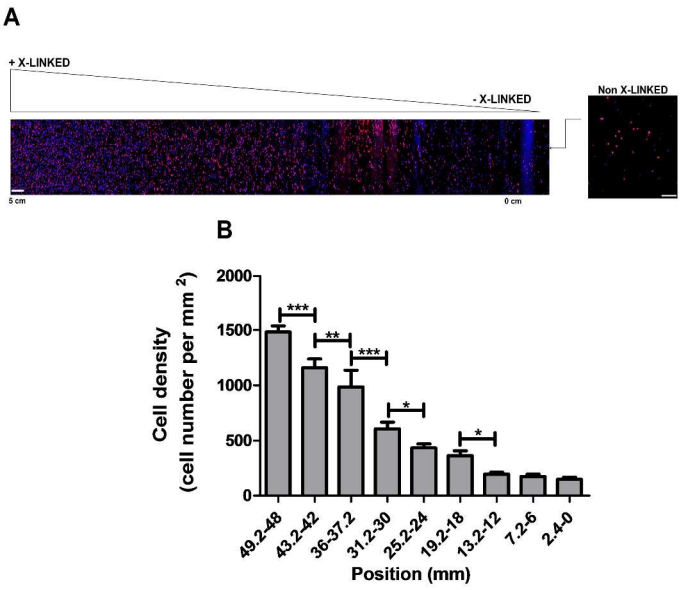

Fig 12. A: DAPI-phallloidin staining of L929 on control (CHIT/ALG multilayers) and on CHIT/ALG multilayers containing a gradient of stiffness along the glass slides. Scale bar is 100 µm for CHIT/ALG multilayers an 1.2 mm for multilayer containing the gradient of stiffness. B: Number of cells attached along the position of the gradient film stiffness. Significant differences were found for (***) $p < 0.001$, (**) $p < 0.01$ and (*) $p < 0.05$.

Conclusions

CHIT/ ALG multilayered films with gradients of physical cues along cm length scale were successfully obtained by controlling genipin cross-linking time using a simple dipping methodology. The results showed that the degree of cross-linking is intrinsically dependent of the reaction time, affecting the surface chemistry as verified by changes on the wettability of the surface. The mechanical properties were evaluated in real time and reveal an increase of the elastic modulus with increasing cross-linking time. Non-conventional local "micro-compression" results confirmed the results obtained directly on freestanding gradient membranes. The cellular properties were also affected by the stiffness gradient. This study suggests that cross-linking deeply modulate not only physicochemical properties but also the cell response, namely in terms of cell adhesion. The present findings highlight the feasibility of LbL to generate stable and tuned modulus gradients that influence the cell-material interactions. Finally, the straightforward method should, in principle, enable us to generate other types of gradients such as: immobilization of bioactive molecules, thickness, swelling and topographic features. The main advantages of this technique are its simplicity and versatility which should allow the process to be translated to other surfaces. Additionally the possibility to easily detach the multilayers upon immersion in water turns the methodology even more attractive.

Acknowledgements

The authors acknowledge the financial support by the Portuguese Foundation for Science and Technology (FCT) through the Doctoral and post-Doctoral grants with the reference numbers SFRH/BD/81372/2011 (JMS), SFRH/BD/73172/2010 (NMO) and SFRH/BPD/96797/2013 (SGC), respectively. This work was financially supported by Foundation for Science and Technology (FCT) by the project PTDC/FIS/115048/2009. The authors would also like to acknowledge the project novel smart and biomimetic materials for innovative regenerative medicine approaches (Ref.: RL1 - ABMR - NORTE-01-0124-FEDER-000016) co-financed by North Portugal Regional Operational Programme (ON.2 – O Novo Norte), under the National Strategic Reference Framework (NSRF), through the European Regional Development Fund (ERDF).

Notes and references

[a] 3B's Research Group – Biomaterials, Biodegradables and Biomimetics, University of Minho, Headquarters of the European Institute of Excellence of Tissue Engineering and Regenerative Medicine, Avepark – Parque de Ciência e Tecnologia, Zona Industrial da Gandra, 4805-017 Barco GMR, Portugal. E-mail: jmano@dep.uminho.pt (J.F.M.)

[b] ICVS/3B's - PT Government Associate Laboratory, Braga/Guimarães, Portugal

†Electronic Supplementary Information (ESI) available. See DOI: 10.1039/c000000x/

1. T. Dvir, B. Timko, D. Kohane and R. Langer, *Nature Nanotechnology*, 2011, **6**, 13–22.
2. K. Ghosh and D. E. Ingber, *Advanced Drug Delivery Reviews*, 2007, **59**, 1306-1318.
3. S. D. Subramony, B. R. Dargis, M. Castillo, E. U. Azeloglu, M. S. Tracey, A. Su and H. H. Lu, *Biomaterials*, 2013, **34**, 1942-1953.
4. A. J. Engler, S. Sen, H. L. Sweeney and D. E. Discher, *Cell*, 2006, **126**, 677-689.
5. F. Rehfeldt, A. J. Engler, A. Eckhardt, F. Ahmed and D. E. Discher, *Advanced Drug Delivery Reviews*, 2007, **59**, 1329-1339.
6. M. S. Kim, G. Khang and H. B. Lee, *Progress in Polymer Science*, 2008, **33**, 138-164.
7. Z. Tang, Y. Wang, P. Podsiadlo and N. A. Kotov, *Advanced Materials*, 2006, **18**, 3203-3224.
8. G. Decher, J. D. Hong and J. Schmitt, *Thin Solid Films*, 1992, **210–211, Part 2**, 831-835.
9. M. M. de Villiers, D. P. Otto, S. J. Strydom and Y. M. Lvov, *Advanced Drug Delivery Reviews*, 2011, **63**, 701-715.
10. C. Detzel, A. Larkin and P. Rajagopalan, *Tissue Engineering Part B: Reviews*, 2011, **17**, 101-113.
11. J. Borges and J. F. Mano, *Chem. Rev.*, 2014, **114**, 8883-8942.
12. K. Ariga, J. P. Hill and Q. Ji, *Physical Chemistry Chemical Physics*, 2007, **9**, 2319-2340.
13. M. Matsusaki, H. Ajiro, T. Kida, T. Serizawa and M. Akashi, *Advanced Materials*, 2012, **24**, 454-474.
14. C. R. Correia, R. L. Reis and J. F. Mano, *Biomacromolecules*, 2013, **14**, 743-751.
15. A. L. Larkin, R. M. Davis and P. Rajagopalan, *Biomacromolecules*, 2010, **11**, 2788-2796.
16. S. G. Caridade, C. Monge, F. Gilde, T. Boudou, J. F. Mano and C. Picart, *Biomacromolecules*, 2013, **14**, 1653-1660.
17. J. M. Silva, A. R. C. Duarte, C. A. Custódio, P. Sher, A. I. Neto, A. C. M. Pinho, J. Fonseca, R. L. Reis and J. F. Mano, *Advanced Healthcare Materials*, 2014, **3**, 433-440.
18. P. Sher, C. A. Custódio and J. F. Mano, *Small*, 2010, **6**, 2644-2648.
19. M. L. Macdonald, R. E. Samuel, N. J. Shah, R. F. Padera, Y. M. Beben and P. T. Hammond, *Biomaterials*, 2011, **32**, 1446-1453.
20. J. Almodovar, T. Crouzier, S. Selimovic, T. Boudou, A. Khademhosseini and C. Picart, *Lab on a Chip*, 2013, **13**, 1562-1570.
21. L. Han, Z. Mao, J. Wu, Y. Guo, T. Ren and C. Gao, *Biomaterials*, 2013, **34**, 975-984.
22. K. Kirchhof, A. Andar, H. B. Yin, N. Gadegaard, M. O. Riehle and T. Groth, *Lab on a Chip*, 2011, **11**, 3326-3335.
23. J. S. Martinez, A. M. Lehaf, J. B. Schlenoff and T. C. S. Keller, *Biomacromolecules*, 2013, **14**, 1311-1320.
24. M. Sailer, K. Lai Wing Sun, O. Mermut, T. E. Kennedy and C. J. Barrett, *Biomaterials*, 2012, **33**, 5841-5847.
25. M. Singh, C. Berkland and M. Detamore, *Tissue Engineering Part B: Reviews*, 2008, **14**, 341-366.
26. N. M. Alves, C. Picart and J. F. Mano, *Macromolecular Bioscience*, 2009, **9**, 776-785.
27. G. V. Martins, E. G. Merino, J. F. Mano and N. M. Alves, *Macromolecular Bioscience*, 2010, **10**, 1444-1455.

28. C. Chaubaroux, E. Vrana, C. Debry, P. Schaaf, B. Senger, J.-C. Voegel, Y. Haikel, C. Ringwald, J. Hemmerlé, P. Lavalle and F. Boulmedais, *Biomacromolecules*, 2012, **13**, 2128-2135.
29. A. L. Hillberg, C. A. Holmes and M. Tabrizian, *Biomaterials*, 2009, **30**, 4463-4470.
30. L. Cui, J. Jia, Y. Guo, Y. Liu and P. Zhu, *Carbohydrate Polymers*, 2014, **99**, 31-38.
31. M. Mekhail, K. Jahan and M. Tabrizian, *Carbohydrate Polymers*, 2014, **108**, 91-98.
32. F. Gaudière, S. Morin-Grognet, L. Bidault, P. Lembré, E. Pauthe, J.-P. Vannier, H. Atmani, G. Ladam and B. Labat, *Biomacromolecules*, 2014, **15**, 1602-1611.
33. N. Bhattarai, J. Gunn and M. Zhang, *Advanced Drug Delivery Reviews*, 2010, **62**, 83-99.
34. J. M. Silva, A. R. C. Duarte, S. G. Caridade, C. Picart, R. L. Reis and J. F. Mano, *Biomacromolecules*, 2014, **15**, 3817-3826.
35. M. V. Voinova, M. Rodahl, M. Jonson and B. Kasemo, *Physica Scripta*, 1999, **59**, 391-396.
36. S. Saha, M. U. Chhatbar, P. Mahato, L. Praveen, A. K. Siddhanta and A. Das, *Chemical Communications*, 2012, **48**, 1659-1661.
37. W.-C. Shen, D. Yang and H. J. P. Ryser, *Analytical Biochemistry*, 1984, **142**, 521-524.
38. K. A. Marx, *Biomacromolecules*, 2003, **4**, 1099-1120.
39. N. G. Hoogeveen, M. A. Cohen Stuart, G. J. Fleer and M. R. Böhmer, *Langmuir*, 1996, **12**, 3675-3681.
40. L. Gao, H. Gan, Z. Meng, R. Gu, Z. Wu, L. Zhang, X. Zhu, W. Sun, J. Li, Y. Zheng and G. Dou, *Colloids and Surfaces B: Biointerfaces*, 2014, **117**, 398-405.
41. F.-L. Mi, H.-W. Sung and S.-S. Shyu, *Journal of Polymer Science Part A: Polymer Chemistry*, 2000, **38**, 2804-2814.
42. H. Chen, W. Ouyang, B. Lawuyi, C. Martoni and S. Prakash, *Journal of Biomedical Materials Research Part A*, 2005, **75A**, 917-927.
43. H. Chen, W. Ouyang, B. Lawuyi and S. Prakash, *Biomacromolecules*, 2006, **7**, 2091-2098.
44. H. G. Sundararaghavan, G. A. Monteiro, N. A. Lapin, Y. J. Chabal, J. R. Miksan and D. I. Shreiber, *Journal of Biomedical Materials Research Part A*, 2008, **87A**, 308-320.
45. K. Madhavan, D. Belchenko and W. Tan, *Journal of Biomedical Materials Research Part A*, 2011, **97A**, 16-26.
46. J. A. Phelps, S. Morisse, M. Hindié, M.-C. Degat, E. Pauthe and P. R. Van Tassel, *Langmuir*, 2010, **27**, 1123-1130.
47. K. Ren, T. Crouzier, C. Roy and C. Picart, *Adv. Funct. Mater.*, 2008, **18**, 1378-1389.
48. T. Crouzier, T. Boudou and C. Picart, *Current Opinion in Colloid & Interface Science*, 2010, **15**, 417-426.
49. J. Almodóvar, L. W. Place, J. Gogolski, K. Erickson and M. J. Kipper, *Biomacromolecules*, 2011, **12**, 2755-2765.
50. S. G. Caridade, E. G. Merino, N. M. Alves and J. F. Mano, *Macromolecular Bioscience*, 2012, **12**, 1106-1113.
51. S. G. Caridade, R. M. P. da Silva, R. L. Reis and J. F. Mano, *Carbohydrate Polymers*, 2009, **75**, 651-659.
52. J. F. Mano, *Macromolecular Bioscience*, 2008, **8**, 69-76.
53. M. Hindié, M. Vayssade, M. Dufresne, S. Quéant, R. Warocquier-Clérout, G. Legeay, P. Vigneron, V. Olivier, J. L. Duval and M. D. Nagel, *Journal of Cellular Biochemistry*, 2006, **99**, 96-104.
54. L. Richert, A. J. Engler, D. E. Discher and C. Picart, *Biomacromolecules*, 2004, **5**, 1908-1916.
55. A. Schneider, C. Vodouhê, L. Richert, G. Francius, E. Le Guen, P. Schaaf, J.-C. Voegel, B. Frisch and C. Picart, *Biomacromolecules*, 2006, **8**, 139-145.
56. O. Semenov, A. Malek, A. Bittermann, J. Vörös and A. Zisch, *Tissue Engineering Part A*, 2009, **15**, 2977-2990.